

AD-A130 143

POTENTIALS AND CHARGES ON CONDUCTING ROCKET SECTIONS
(U) AIR FORCE GEOPHYSICS LAB HANSCOM AFB MA C W DUBS
12 NOV 82 AFGL-TR-82-0349

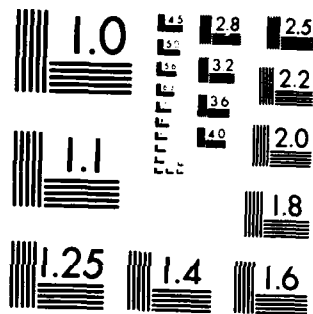
1//

UNCLASSIFIED

F/G 4/1

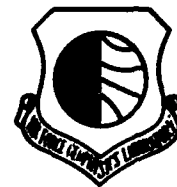
NL

END
DATE
FILMED
8 83
DTIC



AFGL-TR-82-0349

ENVIRONMENTAL RESEARCH PAPERS, NO. 806



(12)

AD A130143

Potentials and Charges on Conducting Rocket Sections

CHARLES W. DUBS

12 November 1982

Approved for public release; distribution unlimited.

DTIC FILE COPY

SPACE PHYSICS DIVISION

PROJECT 7661

AIR FORCE GEOPHYSICS LABORATORY

HANSCOM AFB, MASSACHUSETTS 01731

AIR FORCE SYSTEMS COMMAND, USAF

DTIC
ELECTE
S JUL 7 1983 D

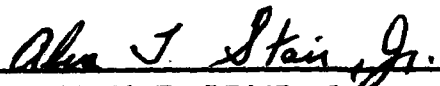
A



88 07 7 086

This report has been reviewed by the ESD Public Affairs Office (PA)
and is releasable to the National Technical Information Service (NTIS).

This technical report has been reviewed and
is approved for publication.


DR. ALVA T. STAIR, Jr.
Chief Scientist

Qualified requestors may obtain additional copies from the
Defense Technical Information Center. All others should apply
to the National Technical Information Service.

1. REPORT NUMBER

2. REPORT DATE (When Data Entered)

REPORT DOCUMENTATION PAGE

READ INSTRUCTIONS BEFORE COMPLETING FORM

1. REPORT NUMBER AFGL TR 82-034	7. GOVT ACCESSION NO.	3. RECIPIENT'S CATALOG NUMBER
4. TITLE AND SUBTITLE POTENTIALS AND CHARGES ON CONDUCTING ROCKET SECTIONS	5. TYPE OF REPORT & PERIOD COVERED Scientific, Interim	6. PERFORMING ORG. REPORT NUMBER ERP No. 805
8. AUTHOR Charles W. Fubs	9. CONTRACT OR GRANT NUMBER	
11. PERFORMING ORGANIZATION NAME AND ADDRESS Air Force Geophysics Laboratory (PHK) Hanscom AFB Massachusetts 01731	10. PROGRAM ELEMENT PROJECT TASK AREA & WORK UNIT NUMBERS 62101F 76611101	
12. CONTROLLING OFFICE NAME AND ADDRESS Air Force Geophysics Laboratory (PHK) Hanscom AFB Massachusetts 01731	12. REPORT DATE 12 November 1982	
14. DISTRIBUTION STATEMENT NAME & ADDRESS (if different from Controlling Office)	13. NUMBER OF PAGES 37	
	15. SECURITY CLASS. (When Reported) Unclassified	
16. DISTRIBUTION STATEMENT (When Reported) Approved for public release; distribution unlimited.		
17. ABSTRACT (Continue on reverse side if necessary; identify by block number) An analysis is made of the potential differences measured by Cohen et al ¹ between pairs of three rocket conductors when various ion or electron beams are emitted. Approximate values of coefficients of potential, capacity, and inductance are calculated. A simple method of measuring them is also presented. Approximate formulas are developed for sheath radius and are used to calculate the minimum and maximum beam currents. The extended probe is found to be most effective at low values of the beam currents except 1 μ A. The potential of the probe is found to be close to zero, so is assumed equal to zero, which		
18. SUPPLEMENTARY NOTES		
19. KEY WORDS (Continue on reverse side if necessary; identify by block number) Potentials Charges Rocket Conductors Beam Current Energy Return current Sheath Charging time constant		
20. ABSTRACT (Continue on reverse side if necessary; identify by block number) An analysis is made of the potential differences measured by Cohen et al ¹ between pairs of three rocket conductors when various ion or electron beams are emitted. Approximate values of coefficients of potential, capacity, and inductance are calculated. A simple method of measuring them is also presented. Approximate formulas are developed for sheath radius and are used to calculate the minimum and maximum beam currents. The extended probe is found to be most effective at low values of the beam currents except 1 μ A. The potential of the probe is found to be close to zero, so is assumed equal to zero, which		

DD FORM 1473

Unclassified

SECURITY CLASSIFICATION OF THIS PAGE (When Data Entered)

Unclassified

SECURITY CLASSIFICATION OF THIS PAGE(When Data Entered)

20. (Contd)

cont → leads immediately to the absolute potentials of the rocket sections. Approximate formulae are developed to calculate the sheath potential from the charge in the sheath. A fast converging reiteration gives the charge on each conductor, the sheath charge, and the part of the conductor potentials that are due to the sheath. Explanations are given for: (1) the charge on the rear section having the opposite sign of, and a smaller magnitude than that on the forward section; (2) the magnitude of the probe voltmeter reading being less than that of the rear section voltmeter for moderate beam currents, and the same for beam currents way beyond saturation; (3) the ratio of these two voltmeter readings approaching 1 with increasing magnitude of beam current; (4) the potential of the probe being negative for ion emission; (5) the magnitude of the probe potential reaching a maximum, then approaching zero with increasing magnitude of beam current. Two different methods are given for calculating the approximate potential of the probe with the probe removed. Calculations of charging time constants show them to be considerably larger than the plasma periods. A few observations are made on the effect of vehicle size and fraction of vehicle surface covered by a dielectric on sheath thickness, vehicle potential, and charge.

1. Cohen, H.A., Sherman, C., and Mullen, E.G. (1979) Spacecraft charging due to positive emission: an experimental study, Geophys. Res. Letts. 6:515

Unclassified

SECURITY CLASSIFICATION OF THIS PAGE(When Data Entered)

Preface

I thank all those who read and commented on an earlier version of this report. I am most grateful to Pradip Bakshi for many discussions, for his reading manuscripts of several different versions of this report, and for much helpful criticism. I thank Allen Rubin for suggesting Table 2, Arthur Besse for fruitful discussion and helpful criticism, William Huber for further experimental information, Kenneth McGee for measuring the capacitance between two rocket sections, and E.G. Mullen for an approximate size of the extended probe.



1. TITLE	2. AUTHOR
3. PERIODICITY	4. DATE
5. DISTRIBUTION STATEMENT	6. SECURITY CLASSIFICATION
7. ABSTRACT	8. NOTES
9. REFERENCES	10. INDEXING TERMS
11. DISTRIBUTION STATEMENT	12. SECURITY CLASSIFICATION
13. ABSTRACT	14. NOTES
15. REFERENCES	16. INDEXING TERMS
17. DISTRIBUTION STATEMENT	18. SECURITY CLASSIFICATION
19. ABSTRACT	20. NOTES
21. REFERENCES	22. INDEXING TERMS
23. DISTRIBUTION STATEMENT	24. SECURITY CLASSIFICATION
25. ABSTRACT	26. NOTES
27. REFERENCES	28. INDEXING TERMS
29. DISTRIBUTION STATEMENT	30. SECURITY CLASSIFICATION
31. ABSTRACT	32. NOTES
33. REFERENCES	34. INDEXING TERMS
35. DISTRIBUTION STATEMENT	36. SECURITY CLASSIFICATION
37. ABSTRACT	38. NOTES
39. REFERENCES	40. INDEXING TERMS
41. DISTRIBUTION STATEMENT	42. SECURITY CLASSIFICATION
43. ABSTRACT	44. NOTES
45. REFERENCES	46. INDEXING TERMS
47. DISTRIBUTION STATEMENT	48. SECURITY CLASSIFICATION
49. ABSTRACT	50. NOTES
51. REFERENCES	52. INDEXING TERMS
53. DISTRIBUTION STATEMENT	54. SECURITY CLASSIFICATION
55. ABSTRACT	56. NOTES
57. REFERENCES	58. INDEXING TERMS
59. DISTRIBUTION STATEMENT	60. SECURITY CLASSIFICATION
61. ABSTRACT	62. NOTES
63. REFERENCES	64. INDEXING TERMS
65. DISTRIBUTION STATEMENT	66. SECURITY CLASSIFICATION
67. ABSTRACT	68. NOTES
69. REFERENCES	70. INDEXING TERMS
71. DISTRIBUTION STATEMENT	72. SECURITY CLASSIFICATION
73. ABSTRACT	74. NOTES
75. REFERENCES	76. INDEXING TERMS
77. DISTRIBUTION STATEMENT	78. SECURITY CLASSIFICATION
79. ABSTRACT	80. NOTES
81. REFERENCES	82. INDEXING TERMS
83. DISTRIBUTION STATEMENT	84. SECURITY CLASSIFICATION
85. ABSTRACT	86. NOTES
87. REFERENCES	88. INDEXING TERMS
89. DISTRIBUTION STATEMENT	90. SECURITY CLASSIFICATION
91. ABSTRACT	92. NOTES
93. REFERENCES	94. INDEXING TERMS
95. DISTRIBUTION STATEMENT	96. SECURITY CLASSIFICATION
97. ABSTRACT	98. NOTES
99. REFERENCES	100. INDEXING TERMS

Contents

1. INTRODUCTION	7
2. COEFFICIENTS OF POTENTIAL, CAPACITY, AND INDUCTION	9
3. NUMERICAL RESULTS	14
4. SUMMARY AND CONCLUSIONS	20
REFERENCES	25
APPENDIX A: Auxiliary Detailed Calculations	27

Illustrations

1. Rocket Diagram	8
A1. Surface Charge Density on Rocket	28
A2. Spherical Conductor and Sheath	32
A3. Cylindrical Conductor and Sheath	33
A4. Cylindrical Conductor and Spherical Sheath	35

Tables

1. Rocket Dimensions in Meters	8
2. Measured Beam Current, Energy, and Conductor Potential Differences	9
3. Sheath Radii, Conductor and Sheath Potentials, Charges, Probe Potentials and Currents, and Charging Time Constants	15

Potentials and Charges on Conducting Rocket Sections

1. INTRODUCTION

Rockets and satellites may become charged to high enough potentials to present a significant problem. A method of controlling the potential is to emit an ion or electron beam. Cohen et al.¹ flew a rocket with three conductors: forward section (1), rear section (2), and extended probe (3) (see Figure 1 and Table 1) to 258 km altitude at night. Conductors 1 and 2 were separated by an insulating ring. At certain times, an ion or electron beam of known current, I_b , and particle energy, E_b , was emitted from the front of the forward section causing certain steady state potentials and charges to develop on the three conductors. Voltmeters measured $\phi_b = V_2 - V_1$ and $\phi_t = V_3 - V_1$. The measurements in Table 2 are part of the results. They are taken from Table 1 and the two extreme points of Figure 5 of Cohen et al.¹ They were measured after steady state was reached, so except for secondary electron current, the return current equals I_b and electrostatic theory is used. An ion beam was emitted with the electron beam, but its current was negligibly small; thus it is ignored in the last line of Table 2. Questions arose: What were the absolute values of the potentials? Why was $\phi_t \sim \phi_b$? Why was $\phi_t < \phi_b$?

(Received for publication 9 November 1982)

1. Cohen, H. A., Sherman, C., and Mullen, E. G. (1979) Spacecraft charging due to positive ion emission: an experimental study, Geophys. Res. Letts. 6:515.

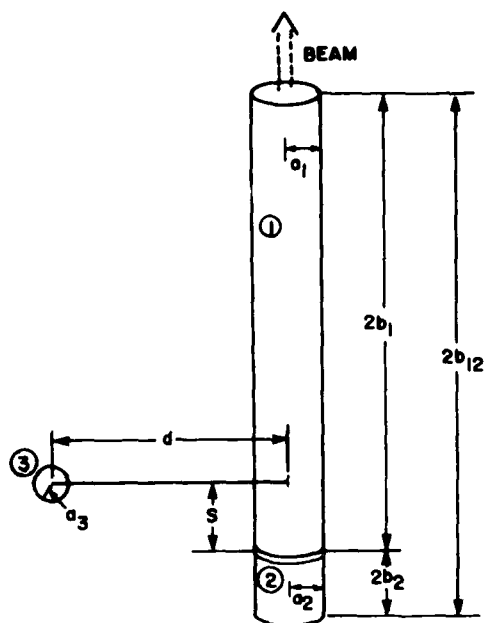


Figure 1. Rocket Diagram

Table 1. Rocket Dimensions in Meters

a_1	a_2	a_3	b_1	b_2	b_{12}	s	d
0.19	0.19	0.07	1.27	0.205	1.475	0.26	1.71

The purpose of this report is to make an approximate analysis of the measurements in Table 2 and to gain an understanding of some of the basic electrical phenomena, including answers to these questions.

First, approximate values of coefficients of potential, capacitance, and inductance are calculated in Section 2. They provide a more complete physical understanding, including (1) the approximate potential the position of the probe would have without the probe, and (2) the charging time constant. Then the sheath radii, absolute potentials of the conductors, part of the latter due to the sheath, charges on the conductors, sheath charge, charging time constant, and ion traverse time through the sheath are calculated and interpreted in Section 3. The summary and conclusions are given in Section 4 and five auxiliary detailed calculations in Sections A1 to A5 of the Appendix.

Table 2. Measured Beam Current, Energy, and Conductor Potential Differences

Beam	I_b μA	E_b keV	ϕ_b kV	ϕ_t kV
ion	1	0.2	0.05	0.02
ion	9	1.0	0.42	0.25
ion	11	2.0		0.47
ion	12	2.0	0.55	0.34
ion	374	2.0		1.04
electron	-10,000	0.09	-0.09	-0.09

2. COEFFICIENTS OF POTENTIAL, CAPACITY, AND INDUCTION

Let p_{ij} , c_{ii} , and c_{ij} for $i \neq j$ be the coefficients of potential, capacity, and induction respectively. Let the subscripts 1, 2, and 3 designate the forward section, the rear section, and the extended probe respectively. From electrostatics, for example, a slight generalization of Page,²

$$V = PQ + V_s, \quad (1)$$

$$Q = C(V - V_s), \quad (2)$$

$$C = P^{-1}, \quad (3)$$

$$V \equiv \begin{bmatrix} V_1 \\ V_2 \\ V_3 \end{bmatrix}, \quad V_s \equiv \begin{bmatrix} V_{1s} \\ V_{2s} \\ V_{3s} \end{bmatrix}, \quad (4), (5)$$

$$P \equiv \begin{bmatrix} p_{11} & p_{12} & p_{13} \\ p_{12} & p_{22} & p_{23} \\ p_{13} & p_{23} & p_{33} \end{bmatrix}, \quad (6)$$

$$Q \equiv \begin{bmatrix} q_1 \\ q_2 \\ q_3 \end{bmatrix}, \quad (7)$$

$$C \equiv \begin{bmatrix} c_{11} & c_{12} & c_{13} \\ c_{12} & c_{22} & c_{23} \\ c_{13} & c_{23} & c_{33} \end{bmatrix}, \quad (8)$$

2. Page, L. (1935) Introduction to Theoretical Physics, Second ed., § 120.

P and C are symmetric, the p_{ij} 's and c_{ii} 's are positive, and the c_{ij} 's for $i \neq j$ are negative. V_{is} is the part of V_i due only to the sheath.

Definitions

- C_1 Capacitance of the forward section by itself.
- C_1' Capacitance of the forward section with the rear section attached, insulated, and uncharged.
- C_{12} Capacitance of the forward and rear sections attached and electrically connected.
- a Radius of a cylinder or a sphere.
- b Half length of a cylinder.

It can be shown that

$$C_1 < C_1' < C_{12} . \quad (9)$$

Smythe³ gave the following empirical formula (here slightly modified to be good to 0.30% instead of 0.41%) for the capacitance of a right circular cylinder of radius a and half length b :

$$c(a, b) = [0.0707 + 0.0615 \left(\frac{b}{a} \right)^{0.76}] a \text{ nf} , \quad (10)$$

a and b in meters. In particular, this gives

$$C_1 = 0.0629_4 \text{ nf} \quad (11)$$

$$C_{12} = 0.0689_0 \text{ nf} . \quad (12)$$

Let us carry out three gedanken experiments, designated with the subscripts a , b , and c . $V_s = 0$ and Eqs. (1), (4), (6), and (7) are used for each. In the first experiment, charge q_{1a} is put on conductor 1 while 2 and 3 are left uncharged. Then

$$V_{1a} = p_{11}q_{1a} \quad (13)$$

$$V_{2a} = p_{12}q_{1a} \quad (14)$$

$$V_{3a} = p_{13}q_{1a} . \quad (15)$$

3. Smythe, W.R. (1962) Charged right circular cylinder, J. Appl. Phys. 33:2966.

Conductor 3 is small and far enough away from conductors 1 and 2 to affect their potentials negligibly, so

$$q_{1a} = C_1 V_{1a} . \quad (16)$$

Eqs. (13) and (16) show that

$$p_{11} = \frac{1}{C_1} . \quad (17)$$

(Dividing Eq. (16) and the top line of Eq. (2) by V_{1a} gives

$$\frac{q_{1a}}{V_{1a}} = C_1^{-1} = c_{11} + c_{12} \frac{V_{2a}}{V_{1a}} + c_{13} \frac{V_{3a}}{V_{1a}} .$$

By dividing Eqs. (14) and (15) by Eq. (13), this becomes

$$C_1^{-1} = c_{11} + c_{12} \frac{p_{12}}{p_{11}} + c_{13} \frac{p_{13}}{p_{11}} ,$$

relating the p_{ij} 's and c_{ij} 's to C_1^{-1} . Multiplying this by p_{11} and using Eq. (17) gives the equation for the top left element of the product CP . Physical consideration shows that $|V_{2a}| < |V_{1a}|$, so Eqs. (13) and (14) show that

$$p_{12} < p_{11} . \quad (18)$$

In the second experiment, charge q_{1b} is put on 1 and q_{2b} on 2 such that $V_{1b} = V_{2b}$ with no charge on 3. Then

$$V_{1b} = p_{11}q_{1b} + p_{12}q_{2b} \quad (19)$$

$$V_{1b} = p_{12}q_{1b} + p_{22}q_{2b} \quad (20)$$

$$V_{3b} = p_{13}q_{1b} + p_{23}q_{2b} . \quad (21)$$

Again, 3 is small and far enough away for V_{1b} to equal $(q_{1b} + q_{2b})C_{12}^{-1}$ accurately. $V_{1b} = (q_{1b} + q_{2b})C_{12}^{-1}$ and $q_{1b} = \lambda q_{2b}$ are substituted into Eqs. (19) and (20). The former may then be written

$$p_{12} = (\lambda + 1)C_{12}^{-1} - \lambda p_{11} . \quad (22)$$

Substituting this into the latter leads to

$$p_{22} = \kappa^2 p_{11} - (\kappa^2 - 1) C_{12}^{-1}. \quad (23)$$

The value of κ is obtained in Section A1 and is Eq. (A10),

$$\kappa = 3.770. \quad (24)$$

Thus, p_{11} , p_{12} , and p_{22} may be obtained given C_1^{-1} .

From Eq. (15),

$$p_{13}^{-1} = \frac{q_{1a}}{V_{3a}}. \quad (25)$$

The value p_{13}^{-1} would have if 2 were missing is shown in Section A2 and is Eq. (A15),

$$p_{130}^{-1} = 0.2659 \text{ nf}. \quad (26)$$

Since 3 is small and far enough away, if 1 and 2 were electrically connected,

p_{13}^{-1} would be

$$\begin{aligned} p_{12,3}^{-1} &= \frac{q_{1b} + q_{2b}}{V_{3b}} \\ &= 0.264_1 \text{ nf}, \end{aligned} \quad (27)$$

Eq. (A16), as also shown in Section A2. (Note the end of Section A2.) It is reasonable to assume that

$$p_{130}^{-1} > p_{13}^{-1} > p_{12,3}^{-1}, \quad (28)$$

similar to Eq. (9). (Actually, $p_{130}^{-1} < p_{13}^{-1} < p_{12,3}^{-1}$.) $V_{3b} = (q_{1b} + q_{2b}) p_{12,3}$ and $q_{1b} = \kappa q_{2b}$ are substituted into Eq. (21), yielding

$$p_{23} = (\kappa + 1) p_{12,3} - \kappa p_{13}. \quad (29)$$

In the third experiment, charge q_{3c} is put on 3 with no charge on 1 or 2. Then

$$V_{3c} = p_{33} q_{3c}. \quad (30)$$

A maximum effect calculation shows that the presence of 1 and 2 changes V_{3c} by less than 3%, so this effect is neglected. Therefore, since the capacitance of 3 is $a_3 \cdot q_{3c} = a_3 V_{3c} g^{-1}$ in MKS units, where $g = 8.98755 \text{ m/nf}$, so that from the value of a_3 in Table 1,

$$p_{33} = \frac{g}{a_3} = 128.4 \text{ (nf)}^{-1}. \quad (31)$$

Thus, all p_{ij} 's may be obtained given C_1^{-1} and p_{13}^{-1} .

Ignoring 3, a good approximation,

$$c_{11} = \frac{p_{22}}{D}, \quad c_{12} = c_{21} = -\frac{p_{12}}{D}, \quad c_{22} = \frac{p_{11}}{D}, \quad (32), (33), (34)$$

$$D = p_{11}p_{22} - p_{12}^2 = (\kappa + 1)^2 C_{12}^{-1} [C_1^{-1} - C_{12}^{-1}]. \quad (35)$$

Choosing $q_2 = -q_1$, the capacity between 1 and 2 is

$$\frac{q_1}{V_1 - V_2} = \frac{c_{11}c_{22} - c_{12}^2}{C_{12}} = \frac{1}{p_{11} - 2p_{12} + p_{22}} = \frac{1}{C_{12}D}. \quad (36)$$

So, as the gap between 1 and 2 approaches 0, this capacity and $|c_{ij}|$ become very large, since C_1^{-1} approaches C_{12}^{-1} . Including 3, as C_1^{-1} approaches C_{12}^{-1} , D approaches 0 and p_{13} approaches $p_{12,3}$.

With Eqs. (9) and (28) in mind, the following reasonable pair of values of effective length of conductor 1 due to 2 being present and of p_{13}^{-1} are chosen:

$$C_1^{-1} = c(a_1, b_1 + b_2/2) = 0.0659_5 \text{ nf}, \quad (37)$$

where $c(a, b)$ is given in Eq. (10), and

$$p_{13}^{-1} = \frac{1}{2}(p_{130}^{-1} + p_{12,3}^{-1}) = 0.265_0 \text{ nf}. \quad (38)$$

These result from using the values in Table 1, Eq. (26), and Eq. (27). The value in Eq. (37) accurately equals the interpolated value, $\frac{1}{2}(C_1 + C_{12})$, from Eqs. (11) and (12). From the above,

$$P = \begin{bmatrix} 15.16 & 12.07 & 3.77 \\ 12.07 & 23.74 & 3.83_5 \\ 3.77 & 3.83_5 & 128.4 \end{bmatrix} \text{ (nf)}^{-1}. \quad (39)$$

From Eqs. (3) and (39),

$$C = \begin{bmatrix} 111.1 & -56.2 & -1.59 \\ -56.2 & 70.7 & -0.462 \\ -1.59 & -0.462 & 7.85 \end{bmatrix} \text{ pf.} \quad (40)$$

Since Eqs. (32) through (35) show that the value of C_1' can be critical, the question naturally arises, "How reasonable is Eq. (37)?" Rocket sections 1 and 2 were separated by a two-in. cylinder of fiberglass which was essentially hollow except for a half-inch thick fiberglass disc. To check, the capacitance between the two ends of an 18.7-cm length of the rocket, which included the gap, was measured and found to be 44.7 pf. A correction due to the missing lengths of 1 and 2 was calculated to be 10.2 pf, probably slightly too large. Adding this and equating to Eq. (36), D is obtained which from Eq. (35) leads to $C_1' = 0.0653$ nf, not far from the value in Eq. (37).

3. NUMERICAL RESULTS

Sheath radii are calculated from Eqs. (A22) and (A23) in Section A3 and are shown in row 3 of Table 3. Using $f_b = f_b(0.7)$ (see the end of Section A3), larger values of R_s are obtained: 1.49 m for $I_b = 1 \mu A$, 3.5% larger than 4.87 m for $9 \mu A$, and smaller percentages larger than the values tabulated for the other beam currents. Note that the probe is inside of the sheath except for the $1 \mu A$ case.

Values of conductor potentials consistent with Table 2 are given in rows 4 to 6 of Table 3. V_2 is set = 0 for reasons given below. The values of V_3 for the $11 \mu A$ cases are guesses. The $374 \mu A$ case is seen¹ to be near or at saturation, the minimum value of $|I_b|$ at which $|V_1| = E_b$, so V_1 is chosen = $-E_b$. The total net charge in the sheath is

$$q_s = -(q_1 + q_2 + q_3). \quad (41)$$

V_s , Q , and q_s are obtained for each value of I_b by successive approximation. First, V_s is guessed. This, V from Table 3, Eqs. (2) and (40) give Q , and Eq. (41) gives q_s . V_s is then calculated from Eqs. (A38) and (A39) in Section A4. Eqs. (A37) and (A32) are used for V_{3s} for $I_b = 1 \mu A$; Eqs. (A35) and (A31) are used for the other cases. The value of b chosen in these equations is $b = b_1 + b_2/2 = 1.3725$ m. These calculations are repeated until self-consistent values are obtained. This procedure converges fairly rapidly for $I_b = 1 \mu A$ and quite rapidly for the other

cases since, for them, $|V_s| \ll |V|$. The results are shown in rows 7 to 13 of Table 3.

Table 3. Sheath Radii, Conductor and Sheath Potentials, Charges, Probe Potentials and Currents, and Charging Time Constants

Row								
1	I_b	1	9	11	11	12	374	-10,000 μA
2	E_b	0.2	1.0	2.0	2.0	2.0	2.0	0.09 keV
3	R_s	1.25	4.87	5.43	5.43	5.70	33.03	11.56 m
4	V_1	-50	-420	-570	-670	-550	-2000	90 V
5	V_2	0	0	0	0	0	0	0
6	V_3	-30	-170	-100	-200	-210	-960	0
7	V_{1s}	36	67	80	95	75	46	-6
8	V_{2s}	36	67	80	95	75	46	-6
9	V_{3s}	20	65	77	92	73	46	-6
10	q_1	-7.4	-50	-67	-79	-65	-223	10.3 nC
11	q_2	2.3	23	31	36	30	112	-5.0
12	q_3	-0.24	-1.04	-0.32	-1.03	-1.19	-4.62	-0.11
13	q_s	5.4	28	37	44	36	116	-5.2
14	V_{33}	-30.7	-134	-41	-132	-153	-593	-14 V
15	$V_3 - V_{33}$	0.7	-36	-59	-68	-57	-367	14
16	I_t	0.67	8.3	16	16	11.3	35	-3 nA
17	I_{r30}		0.93	0.91	0.91	0.90	0.84	-183
18	τ	7.5	5.6	6.2	7.2	5.4	0.60	0.0010 ms
19	$t_t(\tau)$	0.9	2.2			2.4	9.4	0.5
20	$t_t(t_t)$						13.8	1.42

The most striking aspect of these results is that the sign of q_1 is always opposite to, and that of q_2 the same as, that of the beam particles. The reasons are clear. The beam removes charge of one sign, leaving a charge (q_1 after reaching steady state) of the opposite sign. After the beam is turned on, the potential of and charge on the forward section increase in magnitude. Its charge tends to induce a potential of the same sign on the rear section. Both sections therefore attract and collect return plasma particles of the same sign as the beam particles, thus retarding the rise of the magnitude of V_1 and V_2 . Since this current to the rear section is the only current to or from it except voltmeter, secondary electron current, and, for an ion beam, secondary and emitted electrons from the probe, which are negligible or small, this section, 2, gains a charge of the same sign as that of the beam particles. This transient current remains appreciable until V_1 stops changing, that is, until steady state is reached. It flows so as to keep V_2 near zero, that is, so that V_{22} nearly cancels V_{21} . The potential on conductor 1 due to charge q_1 is designated $V_{1j} = p_{1j}q_j$. For positive ion (electron) beam emission, V_2 cannot become appreciably positive (negative) because the return particles lack sufficient energy to cause this. Since the rear section 2, is close to 1 and almost of comparable area, the magnitude of the negative (positive) potential of 2 required to collect enough return current to balance the voltmeter current must be quite small—so it is neglected here, that is, V_2 must be close to zero; here, it is chosen equal to zero. Thus the rear end of the sheath surface must come in close to the rear section. The potentials constant and return current collected by 2 equal to voltmeter current, ϕ_b/Z_b , plus current to the probe emitter, if any, and that due to secondaries from 1, constitute steady state. The voltmeter resistance,⁴ $Z_b = 10^9 \Omega \pm 5\%$. Also, $|q_2| < |q_1|$. Physically, this is due to 1 and 2 not being close enough to each other to be 100% coupled and to 2 being smaller than 1. Mathematically, this is because V_{22} nearly equals $-V_{21}$ and $p_{12} < p_{22}$. The probe, 3, is small and far enough away for $|V_{13}|$ and $|V_{23}|$ to be small, less than 2% of $|V_1|$.

Basically, the same reasoning holds for the extended probe, so $\phi_t \sim \phi_b$. However, since its collecting area is much smaller and it is farther from the front section than the rear section is, with an ion beam not much beyond that for saturation ($\lesssim 1$ mA), the voltmeter current, $I_t = \phi_t/Z_t$, is appreciable. The voltmeter resistance,⁴ $Z_t = 3 \times 10^{10} \Omega \pm 5\%$. Even with the probe emitter and secondary electron current, I_e , to the rear section or outside of the sheath, the probe's steady state potential must be appreciably negative to attract enough return ion current, I_{r3} to equal $I_t - I_e$. Secondaries from 1 to 3 are probably insignificant and are neglected. The potentials constant and $I_t = I_{r3} + I_e$ constitute steady state. Therefore, $\phi_t < \phi_b$. If $q_3 = V_{33} = 0$, V_3 is essentially the probeless potential, that is,

4. Huber, W. B. private communication.

the potential that the position of the extended probe would have if the probe were removed. If $q_p < 0$, $V_p - V_{33}$ is (slightly if $|q_p|$ is small) less negative (or more positive) than the probeless potential. This is due to q_p increasing the positive ion charge density near the probe. Values of V_{33} and $V_p - V_{33}$ are given in rows 14 and 15 of Table 3. Note that $V_p - V_{33}$ is near zero for $I_b = 1 \mu A$ as expected since 3 is outside of the sheath. Using $I_b = I_b(6,7)$ and $E = 0.7$ (see the end of Section A4) results in $q_p = -0.27$ nc and $V_p - V_{33} = 4.7$ V. The latter unphysical value must be due to the pooriness of one or more of the assumptions, probably to the value of I_b and/or E taken. For the other ion beam current cases, $V_p - V_{33}$ is appreciably negative, positive for the electron beam, consistent with the probe being inside of the sheath. The high current electron beam case was so far beyond saturation that the probe potential had to be practically zero for the probe to collect no more return electron current than required to balance $-I_e + I_p$, where I_p is the probe emitter and secondary electron current to the forward section. Thus, for this case, I_e and I_p were negligible. When $q_p - V_{33} = 0$, the probe neither attracts nor repels particles, but, to a rough first approximation, possibly collects I_p times the ratio of the average solid angle the probe subtends at an element of the sheath surface to 2π steradians,

$$I_{p30} = \frac{\pi a_3^2 R_s^2}{2\pi} I_b. \quad (42)$$

The probe radius, $a_3 = 0.07$ m. The displacement, $d = 1.71$ m, of the probe from the center of the sheath makes only 4% error in I_{p30} for $I_b = 9 \mu A$ and less error for higher values of I_b . For comparison, values of I_p and I_{p30} from Eq. (42) are given in rows 16 and 17 of Table 3. I_{p30} is nearly independent of I_b since, from Eq. (A20), R_s^2 is nearly proportional to I_b . $I_{p30} = I_p - I_e$ so is less than I_p . Since I_e is appreciably less than I_p except possibly for the electron beam case, $I_{p30} \approx I_{p30}$ consistent with the signs of the values of V_{33} , row 14, Table 3.

A second, different (not equivalent) way of calculating the approximate probeless potential is as follows. Calculate q_s and V_s for $q_p = 0$. Substitute it and $q_p = 0$ in the bottom line of Eq. (2) and solve for V_3 . For example, for $I_b = 1$ and $9 \mu A$, this procedure gives 0.06 and -39 V as compared to 0.7 and -36 V respectively in row 15 of Table 3.

If I_e were increased from zero to infinity and other given quantities remained constant, the (steady state) value of q_p would go from a maximum magnitude and the same sign as V_1 through zero to a value of smaller magnitude and opposite sign; V_3 would go from V_1 and $-I_e$ from a maximum to practically zero; for an ion beam, I_{p3} and I_e would go from a maximum to zero; for an electron beam, I_e would go from zero to a maximum, $I_{eM} > 0$, and I_{p3} would go from a positive maximum to I_{eM} . For

values of $|I_b|$ approaching saturation potentials and increasing, the (constant) value of Z_t becomes effectively more nearly infinite (I_t more nearly negligible). This is due to I_t becoming a smaller fraction of the total return current with increasing $|I_b|$. This is borne out by the ratio of q_b to q_t in Table 2 being closer to 1 the larger $|I_b|$ is. For $I_b = 374 \mu A$, this ratio from the values in Table 3 is inconsistently large, indicating that the values of V_1 and V_3 shown there are chosen somewhat too negative, and this case was below saturation. As $|I_b|$ increases from zero, $|V_3|$ increases to a maximum near saturation, then approaches zero as $|I_b|$ approaches infinity. What makes the maximum? Beyond saturation, V_1 remains practically constant, the return current increases because it includes the additional beam current, so $|V_3|$ must decrease to increase $|I_t|$. For an ion (electron) beam, q_3 and V_{33} must increase (decrease), eventually changing signs, and the fraction of I_b that the probe collects must decrease (decrease) in order to balance the probe currents. The values in row 6 of Table 3 are consistent with this behavior.

Now the effect of secondary electrons is considered. Let δ be the average number of secondary electrons per primary incident particle. The rocket surface was iridite treated aluminum.⁴ For ion beams below saturation, values of δ for NO^+ on this surface for energies up to 2 keV are needed. In lieu of this, the value used is $\delta = 0.18$, the yield from 1 keV O^+ ions on molybdenum.⁵ The return current, ignoring the small ($\sim 5\% I_b$) voltmeter and emitter currents, even if only a fraction ν ($\sim 2/3$) of the secondaries from 1 exit the sheath, is $I_{r1} = I_b / (1 + \delta)$; so the sheath radii in Table 3 are reduced 8 to 11%. Also, the secondaries decrease the charge density in the vicinity of the rocket thus decreasing q_s and increasing q_1 (decreasing $|q_1|$). V_1 may increase slightly except at or above saturation. The other $1 - \nu$ of the secondaries goes to conductor 2. About $0.11 I_r$ must return to 2 to balance this $\sim 0.06 I_r$ secondary, $\sim 0.05 I_r$ 2 to 1 voltmeter current, and $-0.04 I_r$ to 0 current due to secondaries from 2. A more complicated, complete theory is required for a more detailed and accurate description.

The amount and effect of secondary electrons in the electron beam case is much different. Using the formula of Sternglass⁶ and the values for aluminum:⁵ $\delta_{max} = 0.97$ and $U_{max} = 300 V$, the value $\delta = 0.72$ is obtained for $U = 90 V$. Thus many secondary electrons must be generated by the return electrons hitting the forward section. Since they have no more than a few eV energy, however, they

5. Stannard, P. R., Katz, I., Mandell, M. J., Cassidy, J. J., Parks, D. E., Rotenberg, M., Steen, P. G. (1980) Analysis of the charging of the SCATHA (P78-2) satellite, Report NASA CR-165348, SSS-R-81-4798, pp 22-24, 29.

6. Sternglass, E. J. (1954) Backscattering of kilovolt electrons from solids, Phys. Rev. 95:345.

do not escape, but, in steady state, must be collected by the forward section as fast as they are generated. Therefore, the sheath radius is not changed by the production of secondaries, and the return electron current (including returning beam electrons if above saturation) equals the beam current. If above saturation, V_1 cannot be affected. The only essential effects of the secondaries are (1) to increase the electron density near the forward section, causing the electric field to be larger than otherwise near the forward section and smaller in the outer part of the sheath, and (2) to increase q_1 and thus $|q_s|$. Other electrical quantities may change slightly. Some of the return electrons will scatter instead of being collected, causing the sheath radius to increase. This is believed to be a small effect with this rocket and is not treated here.

Ionization by beam and return ions is negligible due to the small ion speeds and high ionization threshold energy. For the $I_b = -10$ mA case, however, both the beam and return electrons produce ionization near the rocket. This has the effect of decreasing q_1 , increasing the charge density (decreasing $|\rho|$) near the rocket, and thus of decreasing $|q_s|$. V_1 is unaffected since $|I_b|$ is much greater than the saturation value. Ionization at 140 - 150 km altitude has a moderate effect at most since the minimum ionization mean free path there is about 1000 to 2000 m.

The charging time constant, τ , of the forward section is calculated and compared to the plasma periods. For the charge density, $n_0 = 10^3 \text{ cm}^{-3}$, the latter are 0.76 ms and 3.5 μs for ions and electrons respectively. The former may be calculated approximately as follows. For simplicity, the probe is ignored since it has only a small effect, the small voltmeter current is neglected, and the ion transit time is assumed to be much smaller than τ . Let the instantaneous and final values respectively of conductor minus sheath potential at conductor 1 be x and $X = V_1 - V_{1s}$, at conductor 2 be $-v_{2s}$ and $-V_{2s}$, and of forward section return current be i_{r1} and I_{r1} . From the top line of Eq. (2),

$$q_1 = c_{11}x - c_{12}v_{2s}. \quad (43)$$

$$\frac{dq_1}{dt} = i_{r1} + \delta i_{r1} - I_b = c_{11} \frac{dx}{dt} - c_{12} \frac{dv_{2s}}{dt}. \quad (44)$$

The assumption is made that

$$i_{r1} = \frac{x}{X} I_{r1} = \frac{I_b}{(1 + \delta)X} x \text{ and } v_{2s} = \frac{x}{X} V_{2s}. \quad (45), (46)$$

7. Leadon, R.E., Woods, A.J., Wenaas, E.P., and Klein, H.H. (1981)
Analytical Investigation of Emitting Probes in an Ionized Plasma,
 AFGL-TR-81-0138, AD A104166.

Then

$$\frac{dv_{2s}}{dt} = \frac{V_{2s}}{X} \frac{dx}{dt} \text{ and } [c_{11} - c_{12} \frac{V_{2s}}{X}] \frac{dx}{dt} = -I_b (1 - \frac{x}{X}). \quad (47), (48)$$

Assuming $x = 0$ at $t = 0$ when the beam is turned on, the solution of Eq. (48) is

$$x = X \left[1 - e^{-\frac{t}{\tau}} \right], \quad (49)$$

$$\tau = - \frac{c_{11}(V_1 - V_{1s}) + c_{12}V_{2s}}{I_b}. \quad (50)$$

Values of τ from Eq. (50) are given in row 18 of Table 3. Thus, the charging time constant is large compared to the plasma period for ion beam currents, $I_b \leq 12 \mu A$, but not for the largest ion beam current or the electron beam current. As a check, the approximate time, t_t , for an NO^+ ion to traverse the sheath radially, starting at $t = 0$, is calculated for each beam current except $11 \mu A$ (see Section A5). For ion beams, the ion is assumed to start at the sheath boundary with velocity v_t in the $-\vec{r}$ direction; for the electron beam, the ion is assumed to start at the conductor with zero velocity. Values of t_t for charging time constants $\tau' = \tau$ and $t_t > \tau$ are shown in rows 19 and 20 respectively of Table 3. The charging time constant due to capacitances is seen to be much larger than the ion transit time and thus solely determines the time for steady state to be reached only for the $1 \mu A$ case. The time to reach steady state is determined by both the capacitances and the ion transit time for the 9 and $12 \mu A$ cases, and essentially solely by the ion transit time for the $374 \mu A$ and $-10 mA$ cases.

4. SUMMARY AND CONCLUSIONS

An analysis is made of measurements of potential differences between pairs of three conductors (two rocket sections and an extended probe) flown in the night-time ionosphere when an ion or electron beam was emitted from the forward section.¹

Approximate values of coefficients of potential (and thus coefficients of capacity and induction) can be calculated without using complicated potential theory for the conductors of an object which has a fairly simple geometry. These coefficients are calculated for the forward section (1), rear section (2) and extended probe (3) of the rocket described in Cohen et al.¹ Reasonable choices of the limited values of two parameters are sufficient to give the value of the P matrix which is inverted

to give the C matrix. A measurement of capacity between the forward and rear sections confirms that the important parameter is chosen approximately correctly. The magnitudes of c_{13} , c_{23} , and c_{33} are much smaller than those of the other c_{ij} 's since the probe was small and far enough away from the other conductors to interact with them only weakly. P could also be measured as follows. Hang the rocket away from other conductors > 10 m above ground and run a small ground wire, 0, up to the rocket. Measure the capacities between 1 and 0, 2 and 0, 3 and 0, 1 and 2, 2 and 3, and 3 and 1. The first three measurements give the p_{ii} 's, and the last three give the p_{ij} 's for $i \neq j$. The effect of using more accurate values of the c_{ij} 's than those used in this report is expected to be small.

A formula is developed for a cylindrical sheath radius and for interpolation between it and the spherical sheath radius to give approximate sheath radii for the various beam currents considered. The probe is found to be inside of the sheath except for the beam current, $I_b = 1 \mu A$.

The potential of the rear section is shown to be close to zero. It is chosen equal to zero, which, with the potential differences, determines the absolute potentials. An investigation of how close V_2 is to zero would be interesting. It is slightly negative (positive) for ion (electron) beams.

The total net sheath charge is the negative of the sum of the charges on the three rocket conductors. Formulae are developed to give the sheath potential as a function of this charge, the sheath radius, and the radius of the point in the sheath. The sheath charge density is assumed constant. These formulae are used to give the part of the conductor potentials that is due only to the sheath. The latter and the conductor charges are determined by a fast converging reiteration. Except for $I_b = 1 \mu A$, the sheath potentials are relatively small. Nevertheless, use of Jaycor's more realistic simplified Lam sheath treatment⁷ instead of assuming constant charge density would be interesting and not very difficult, to ascertain that this more correct treatment would make only a small correction.

The charge on the rear section is always positive for a positive ion beam, negative for an electron beam, and of smaller magnitude than that on the forward section. The rear to forward section voltmeter current and any probe emitter electron current to the rear section have a negligible effect.

The extended probe has a much smaller area and is farther from the forward section than the rear section is, so it collects much less return current for a given potential. This and the size of the probe to forward section voltmeter resistance cause V_3 to be between 0 and V_1 , except for beam currents far beyond saturation, the minimum value of I_b for which $|V_1| = E_b$, the beam particle energy. Thus, in general, $|\phi_t| < |\phi_b|$. This resistance is so low that, for all the positive ion beam ($I_b > 0$) cases considered, the charge on the probe, q_3 , must be negative for

the probe and emitter current to balance the voltmeter current. For $I_b > 0$, much larger values of this resistance and/or I_b would cause q_3 to be positive. For $|I_b|$ beyond saturation and increasing, this voltmeter current becomes more nearly negligible and $|V_3|$ approaches zero. With the voltmeter used, as $|I_b|$ increases from zero, at first $|V_3|$ increases and ϕ_t/ϕ_b is a positive number appreciably less than one. After saturation is approached, $|V_3|$ reaches a maximum then approaches 0 (except for thermal energy) while ϕ_t/ϕ_b approaches 1. The numbers in Tables 2 and 3 are consistent with these conclusions, but more extensive data to test them would be desirable. Since the electron beam case is way beyond saturation, the probe to forward section voltmeter resistance is effectively infinite.

If $q = 0$, the probeless potential, that is, the potential at the position of the probe with the probe removed, is essentially V_3 . Two non-equivalent methods are given for calculating the approximate probeless potential when $q_3 \neq 0$.

For a positive ion beam, secondaries reduce the sheath size, decrease the charge density near the rocket, q_s , and $|q_1|$. For an electron beam, many secondaries may be produced which increase the electron density near the forward section. Their effect is to increase the electric field near the rocket, to decrease the field in the outer part of the sheath, to increase q_1 and $|q_s|$, and, if below saturation, to increase slightly the rocket potential. Further investigation would be interesting. The effect of scattering is thought to be small but should be investigated.

Ionization is negligible for positive ion beams, but should be investigated for electron beams, for which it has a small or moderate effect.

The charging time constant of the rocket (the forward section) due to its capacitance is calculated for each value of I_b . It is much larger than the ion plasma period for ion beam currents less than a few 10's of μA . It dominates the time behavior below $\sim 10 \mu A$ ion beam current. The ion transit time through the sheath becomes important at higher beam currents and dominates the time behavior at ion and electron beam currents near or above saturation.

A number of approximations are used in this report. More accurate treatments would lead to appreciable changes in numerical results, but they would be expected to make little or no qualitative changes. A combination of the capacitive coupling equations used here and a more complete probe theory may lead to a prediction of the potentials and charges on the conductors of a rocket or satellite such as that considered here. The treatment here for three conductors may easily be extended to any number of isolated conductors or small insulators of a rocket or satellite.

From the results of Lam-Jaycor⁷ and this report, one may induce the following general steady state properties of vehicles in the ionosphere at potentials small enough not to cause breakdown and appreciable ionization of background neutrals. For a given beam current and shape of vehicle with an all-conducting surface, as

the size increases, the sheath thickness, vehicle potential, and charge decrease. For sheaths that are thick compared to vehicle size, the charge decreases very little. For a given beam current and vehicle, as the fraction of the surface that is covered with dielectric is increased, the potential and charge on the conducting part increase.

After this report was written, my attention was drawn to a paper by Katz and Mandell,⁸ who made some analysis of the rocket of Cohen et al.¹ They concluded from their calculations that the rear section is no more than 1 V negative when the forward section is charged negatively to several kV in a plasma with a fraction of an eV temperature. They indicated that this potential would be positive and of larger magnitude when the forward section is positively charged over a kV, but did not consider the case of its potential $\sim +100$ V. They also concluded that the forward section potential was nearly saturated at -2 kV for $I_b = 374 \mu A$ ($\sim 400 \mu A$). Their explanation of the difference in probe and rear section potentials, however, disagrees with that in the present report. They seem not to have considered the important effects of the charge on the probe and the probe to forward section voltmeter current.

8. Katz, I., and Mandell, M. J. (1982) Differential charging of high-voltage spacecraft: the equilibrium potential of insulated surfaces, J. Geophys. Res. 87:4533.

References

1. Cohen, H. A., Sherman, C., and Mullen, E.G. (1979) Spacecraft charging due to positive ion emission: an experimental study, Geophys. Res. Letts. 6:515.
2. Page, L. (1935) Introduction to Theoretical Physics, Second ed., §120.
3. Smythe, W.R. (1962) Charged right circular cylinder, J. Appl. Phys. 33:2966.
4. Huber, W.B. private communication.
5. Stannard, P.R., Katz, I., Mandell, M.J., Cassidy, J.J., Parks, D.E., Rotenberg, M., Steen, P.G. (1980) Analysis of the charging of the SCATHA (P78-2) satellite, Report NASA CR-165348, SSS-R-81-4798, pp 22-24, 29.
6. Sternglass, E.J. (1954) Backscattering of kilovolt electrons from solids, Phys. Rev. 95:345.
7. Leadon, R.E., Woods, A.J., Wenaas, E.P., and Klein, H.H. (1981) Analytical Investigation of Emitting Probes in an Ionized Plasma, AFGL-TR-81-0138, AD A104166.
8. Katz, I., and Mandell, M.J. (1982) Differential charging of high-voltage spacecraft: the equilibrium potential of insulated surfaces, J. Geophys. Res. 87:4533.

Appendix A

Auxiliary Detailed Calculations

A1. FORWARD TO REAR SECTION CHARGE RATIO

In this section, the ratio k of the charge on the forward section of the rocket to that on the rear section when the two sections are electrically connected is calculated.

From Smythe,³ the surface charge density on the side and end respectively are

$$\sigma_s = \sum_{n=0}^{N_s} A_n \left(1 - \frac{z^2}{b^2}\right)^{n-1/3} \quad (A1)$$

$$\sigma_e = \sum_{n=0}^{N_e} B_n \left(1 - \frac{R^2}{a^2}\right)^{n-1/3} \quad (A2)$$

$$q_1 = q_{s1} + q_e \quad (A3)$$

$$q_2 = q_{s2} + q_e \quad (A4)$$

$$q_{si} = 2 \pi a \left[\int_0^b -(-1)^i \int_0^{b-2b_2} \right] \sigma_s dz. \quad (A5)$$

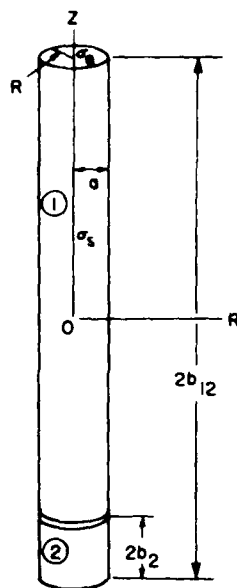


Figure A1. Surface Charge Density on Rocket

Let $z = by^{1/2}$. Then Eq. (A5) becomes

$$q_{si} = \pi ab \sum_{n=0}^{N_s} A_n \left[\int_0^1 -(-1)^i \int_0^{(1-\frac{2b_2}{b})^2} (1-y)^{n-1/3} y^{-1/2} dy \right] \quad (A6)$$

The first integral is a beta function,

$$\int_0^1 (1-y)^{n-1/3} y^{-1/2} dy = \frac{\Gamma(1/2) \Gamma(n+2/3)}{\Gamma(n+7/6)} \quad (A7)$$

These gamma functions are known or may easily be determined accurately.

$$2b_2 = 0.41 \text{ and } b = b_{12} = 1.475 \text{ m ,}$$

so

$$(1 - \frac{2b_2}{b})^2 = 0.521333 \quad (A8)$$

The second integral in Eq. (A6) was evaluated by expanding the binomial, integrating term by term, and keeping as many terms as necessary for accuracy. Since

$b = 7.76a$, the values of A_n and B_n given in Smythe³ for $b = 8a$ were used.
 $N_s = 4$ and $N_e = 0$.

$$q_e = \int_0^a \sigma_e 2\pi R dR = \frac{3}{2} \pi B_0 a^2. \quad (A9)$$

Using $a = 0.19$ m, finally

$$\kappa = \frac{q_1}{q_2} = 3.77024. \quad (A10)$$

(Assuming a constant surface charge density would have given the erroneous value 5.22 for κ .)

A2. AN EMPIRICAL FORMULA FOR THE POTENTIAL NEAR A RIGHT CIRCULAR CYLINDER

The following empirical formula is developed for the potential at a point R, z (see Figure A1) due to a right circular cylinder with a charge Q .

$$V = \frac{kQ}{a} \left[\left(1 + \frac{b}{R \sqrt{1 + \frac{z^4}{b^4 + R^2 z^2}}} \right)^{\frac{a}{kb} - 1} - 1 \right] g, \quad (A11)$$

a in meters, Q in Coulombs, V in Volts, $g = 8.98755$ m/nf.
 When $b \ll |z|$ and $b^2 \lesssim R|z|$,

$$V = \frac{Q}{R \sqrt{1 + \frac{z^4}{b^4 + R^2 z^2}}} g. \quad (A12)$$

When $(b \ll |z| \text{ and } b \lesssim R) \text{ or } b \ll R$,

$$V = \frac{Q}{\sqrt{R^2 + z^2}} g. \quad (A13)$$

When $\frac{R}{b} \ll \ln \frac{b}{R} \ll \frac{2kb}{a}$ and $|z| \lesssim b$,

$$V = \frac{Q}{b} \left[\ln \frac{b}{R \sqrt{1 + \frac{z^4}{b^4}}} \right] g. \quad (A14)$$

When $z = 0$, $R = a$, $k = 1.777$, and $a/2 < b \leq 8a$, then Q/V is within 1.25% of the correct capacitance.

p_{130}^{-1} is Q/V obtained from Eq. (A11) with $a = 0.19$ m, $k = 1.777$, $b = 1.27$ m, $R = 1.71$ m, $|z| = 1.01$ m, giving

$$p_{130}^{-1} = 0.265_9 \text{ nf.} \quad (\text{A15})$$

$p_{12,3}^{-1}$ is Q/V obtained from Eq. (A11) with $a = 0.19$ m, $k = 1.777$, $b = 1.475$ m, $R = 1.71$ m, $|z| = 0.805$ m, giving

$$p_{12,3}^{-1} = 0.264_1 \text{ nf.} \quad (\text{A16})$$

Physical consideration indicates that this should be larger than Eq. (A15). This discrepancy is due to some inaccuracy in Eq. (A11). The latter may be improved by replacing b^4 by $2b^4$. This leads to $p_{130}^{-1} = 0.260_5 \text{ nf}$ and $p_{12,3}^{-1} = 0.261_6 \text{ nf}$. Use of these values instead of Eqs. (A15) and (A16) would make little change.

A3. SHEATH RADIUS

In this section, an approximate interpolation formula for sheath radius is developed.

Leadon et al⁷ used a modification (simplification) of Lam's method to obtain the radius, r_s , of the spherical sheath around an emitting probe. They equated the thermal current density times the sheath area to the beam current. This gives

$$r_s = \sqrt{\frac{I_r}{4 \pi |q| n_o v_t}}. \quad (\text{A17})$$

I_r is the return current usually taken equal to I_b , q is the charge, v_t the modified thermal speed $\sqrt{\frac{kT}{2 \pi m}}$, and m the mass of the return particles.

The ion to electron mass ratio is taken to be 46,000. k is Boltzmann's constant, the plasma temperature, T , is taken to be 550°K, and the number density, n_o , to be 10^9 m^{-3} . Eq. (A17) is valid when r_s is large compared to probe (rocket) size.

When the outside of the sheath is close to the rocket, the sheath is assumed to be a cylinder concentric with the rocket. Similarly, the return current is equated to thermal current density times the sheath area

$$I_r = (2 \pi R_s^2 + 2 \pi R_s 2B) n_o |q| v_t. \quad (\text{A18})$$

where R_s is the sheath radius and B is half the sheath length. The latter is assumed to be

$$B = (b/a)R_s. \quad (A19)$$

So the sheath radius is assumed to be

$$R_s = \sqrt{\frac{f I_r}{2 \pi n_o |q| v_t}}. \quad (A20)$$

For small beam currents, $f = \frac{a}{2b+a}$; for large beam currents, $f = \frac{1}{2}$. The interpolation factor is taken to be

$$f = \frac{(x + I_r)a}{(2b+a)x + 2aI_r}. \quad (A21)$$

Somewhat arbitrarily, x is chosen so that $f = f_b = f_b(0.5) \equiv \frac{1}{2}(\frac{1}{2} + \frac{a}{2b+a})$ when $R_s = b$. Eq. (A20) is solved for $I_r = I_{rb}$ when $R_s = b$ and $f = f_b$. Then Eq. (A21) is solved for x when $f = f_b$ and $I_r = I_{rb}$. This leads to

$$R_{si} = \sqrt{\frac{I_r(I_r + 0.148)}{0.342(I_r + 1.14)}} \quad (A22)$$

for an ion beam, and

$$R_{se} = \sqrt{\frac{|I_r|(|I_r| + 31.7)}{73.3(|I_r| + 244.6)}} \quad (A23)$$

for an electron beam, where R_s is in meters and I_r in μA . The values of R_s in Table 3 are calculated from Eqs. (A22) and (A23). Values are also calculated the same way but with $f_b = f_b(0.7) \equiv 0.3 \times \frac{1}{2} + 0.7 \times \frac{a}{2b+a}$.

A4. THE POTENTIAL DUE TO THE SHEATH

For simplicity, the sheath charge density ρ_s is assumed constant in this first treatment of the sheath.

First, suppose a spherical conductor of radius a and charge $-q_s$ surrounded by a spherical sheath of radius r_s and total charge q_s (Figure A2).

$$\frac{4}{3} \pi (r_s^3 - a^3) \rho = q_s. \quad (\text{A24})$$

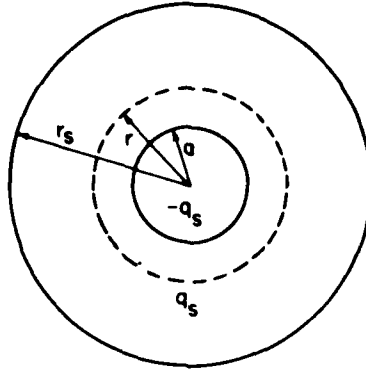


Figure A2. Spherical Conductor and Sheath

From Gauss's Law, for $a \leq r < r_s$,

$$4 \pi r^2 E = 4 \pi [-q_s + \frac{4}{3} \pi (r^3 - a^3) \rho] g, \quad (\text{A25})$$

where E is the (radial) electric field at a radial distance r . The potential, V , at r minus the potential there due to the conductor is the potential due to the sheath,

$$V_s = V - V_a = \int_r^{r_s} E(r') dr' + \frac{q_s g}{r} = \frac{q_s g}{r_s^3 - a^3} \left[\frac{3r_s^2 - r^2}{2} - \frac{a^3}{r} \right]. \quad (\text{A26})$$

Secondly, the potential is obtained in the median plane, $z = 0$, due to a cylindrical sheath of radius R_s and half length $B = (b/a)R_s$ of charge q_s surrounding a cylindrical conductor of radius a and half length b (Figure A3). First, the case of $R \leq R_s$ is treated. Eq. (A11) is used with, for simplicity, $z = 0$. The potential at R due to an infinitesimal shell at $R' \leq R$ and $z' \leq z$ is

$$dV_{<} = \frac{k dq_s g}{R'} \left[\left(1 + \frac{z'}{R}\right)^{\frac{R'}{kz'}} - 1 \right]. \quad (\text{A27})$$

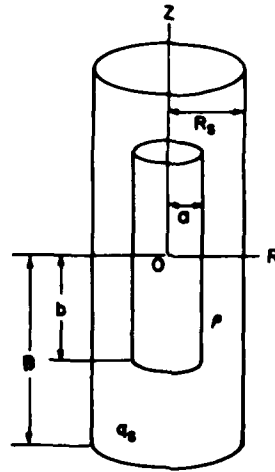


Figure A3. Cylindrical Conductor and Sheath

The potential at R due to a similar shell at $R' \geq R$ and $z' \geq z$ is assumed independent of R , so is

$$dV_{>} = \frac{k dq_s g}{R'} \left[\left(1 + \frac{z'}{R'} \right)^{\frac{R'}{kz'}} - 1 \right]. \quad (\text{A28})$$

To make the exponent constant and thus the potential integrable, z' is taken $= (b/a)R'$. The charge density is q_s divided by the sheath volume,

$$\rho = \frac{aq_s}{2\pi b(R_s^3 - a^3)}. \quad (\text{A29})$$

$$dq_s = \rho [2\pi R' 2z' dR' + 2\pi R'^2 dz'] = \frac{3q_s R'^2}{R_s^3 - a^3} dR'. \quad (\text{A30})$$

Thus, the potential due to the sheath at a point R inside the sheath is

$$\begin{aligned}
V_{sc}^i(R) &= \int_a^R dV_{<} + \int_R^{R_s} dV_{>} \\
&= \frac{3kq_s g}{R_s^3 - a^3} \left\{ \frac{aR \left[R \left(1 + \frac{b}{a}\right)^{\frac{a}{kb} + 1} - a \left(1 + \frac{b}{R}\right)^{\frac{a}{kb} + 1} \right]}{b \left(\frac{a}{kb} + 1\right)} \right. \\
&\quad \left. - \frac{a^2 R^2 \left[\left(1 + \frac{b}{a}\right)^{\frac{a}{kb} + 2} - \left(1 + \frac{b}{R}\right)^{\frac{a}{kb} + 2} \right]}{b^2 \left(\frac{a}{kb} + 1\right) \left(\frac{a}{kb} + 2\right)} \right. \\
&\quad \left. - \frac{1}{2}(R^2 - a^2) + \frac{1}{2} \left[\left(1 + \frac{b}{a}\right)^{\frac{a}{kb}} - 1 \right] (R_s^2 - R^2) \right\}. \tag{A31}
\end{aligned}$$

This reduces to Eq. (A26) for $b = a$ and $k = 1$. For the case $R \geq R_s$, using Eq. (A27),

$$\begin{aligned}
V_{sc}^o(R) &= \int_a^{R_s} dV_{<} \\
&= \frac{3kq_s g}{R_s^3 - a^3} \left\{ \frac{aR}{b \left(\frac{a}{kb} + 1\right)} \left[R_s \left(1 + \frac{bR_s}{aR}\right)^{\frac{a}{kb} + 1} - a \left(1 + \frac{b}{R}\right)^{\frac{a}{kb} + 1} \right] \right. \\
&\quad \left. - \frac{aR}{b \left(\frac{a}{kb} + 2\right)} \left\{ \left(1 + \frac{bR_s}{aR}\right)^{\frac{a}{kb} + 2} - \left(1 + \frac{b}{R}\right)^{\frac{a}{kb} + 2} \right\} \right] \\
&\quad \left. - \frac{R_s^2 - a^2}{2} \right\}. \tag{A32}
\end{aligned}$$

As $R \rightarrow \infty$, $V_{sc}^o \rightarrow \frac{q_s g}{R}$ as it must.

For increasing $R_s \gg b$, the sheath surface becomes spherical. So, the potential due to such a sheath at point R in the median plane is calculated. It is the potential due to the sphere of uniform charge density ρ minus that due to the cylinder a, b of density ρ . First, this potential for $R \leq R_s$ is calculated.

$$V_{ss}^i(R) = \frac{\frac{4}{3}\pi R_s^3 \rho g}{R_s} + \int_R^{R_s} \frac{\frac{4}{3}\pi R'^3 \rho g}{R'^2} dR' - V_c. \tag{A33}$$

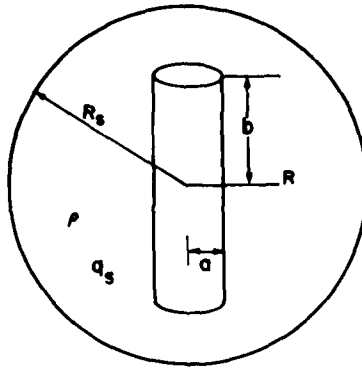


Figure A4. Cylindrical Conductor and Spherical Sheath

V_c is given by Eq. (A32) in the limit of $a \rightarrow 0$ at constant b/a , then R_s is replaced by \underline{a} and q_s by $\pi a^2 2b\rho$.

$$\left(\frac{4}{3}\pi R_s^3 - \pi a^2 2b\right) \rho = q_s. \quad (\text{A34})$$

So, Eq. (A33) becomes

$$V_{ss}^i(R) = \frac{q_s g}{R_s^3 - \frac{3}{2}a^2 b} \left\{ \frac{3R_s^2 - R^2}{2} - X \right\}, \quad (\text{A35})$$

$$X = \frac{9}{2}kab \left\{ \frac{R}{b(\frac{a}{kb} + 1)} \left[\left(1 + \frac{b}{R}\right)^{\frac{a}{kb} + 1} - \frac{R}{b(\frac{a}{kb} + 2)} \left\{ \left(1 + \frac{b}{R}\right)^{\frac{a}{kb} + 2} - 1 \right\} \right] - \frac{1}{2} \right\}. \quad (\text{A36})$$

If $k = 1$ and $b = a$, this reduces to Eq. (A26) with a^3 replaced by $(3/2)a^3$. If $k = 3/2$ and $b = (2/3)a$, Eq. (A35) reduces to Eq. (A26). Secondly, the potential due to the sheath at $R \geq R_s$ is

$$V_{ss}^o(R) = \frac{\frac{4}{3}\pi R_s^3 \rho g}{R} - V_c = \frac{q_s g}{R_s^3 - \frac{3}{2}a^2 b} \left[\frac{R_s^3}{R} - X \right]. \quad (\text{A37})$$

As $r \rightarrow \infty$, $V_{ss}^0 \rightarrow \frac{q_s g}{R}$ as it must.
The sheath potential is taken as

$$V_s(R) = F V_{ss} + (1 - F) V_{sc}, \quad (A38)$$

both for $R \leq R_s$ and $R \geq R_s$. $F \rightarrow 1$ as $R_s \rightarrow \infty$, and $F \rightarrow 0$ as $R_s \rightarrow a$. So, the interpolation factor is taken to be

$$F = \frac{R_s - a}{R_s + y}. \quad (A39)$$

Somewhat arbitrarily, y is chosen so that $F = F_b = 0.5$ when $R_s = b$. Then, $y = b - 2a$. The same calculation is also made with $f_b = f_b(0.7)$ and $F_b = 0.7$, for which $y = (3b - 10a)/7$.

A5. ION TRAVERSE TIME THROUGH THE SHEATH

For simplicity, the traverse time is taken to be the time calculated for an ion to move radially through a sheath around a charging spherical conductor, starting when the beam is turned on at $t = 0$. The beam current rise time is assumed to be much shorter than this traverse time. Also, the assumption is made that the field grows exponentially with time and the radial dependence of field and potential are independent of time. The radial acceleration of an ion of charge e and mass M is

$$\frac{d^2 r}{dt^2} = \frac{e}{M} E. \quad (A40)$$

The values of e and M taken are the magnitude of the electron charge and the mass respectively of an NO^+ ion. From Eqs. (A24), (A25), (A40) and the time assumption,

$$\frac{d^2 r}{dt^2} = - \frac{eq_s g}{M(r_s^3 - a^3)} \left[\frac{r_s^3}{r^2} - r \right] \left[1 - e^{-\frac{t}{\tau}} \right]. \quad (A41)$$

The value of r_s is taken from row 3 of Table 3. Integrating E from a to r_s at $t = \infty$ leads to

$$V(a) = - \frac{q_s g}{a} \cdot \frac{r_s^2 - (r_s - a)a/2}{r_s^2 + r_s a + a^2}. \quad (A42)$$

The value of a is chosen so that $V(a)$ equals the value in row 4 of Table 3. This results in $0.47 < a < 0.51$ m.

For an ion beam, at $t = 0$: $r = r_s$ and $dr/dt = -v_t$. From Section A3 $v_t = 156$ m/s. The mass is taken to be that of NO^+ . The traverse time, t_t , is the time at which $r = a$. For the electron beam, at $t = 0$: $r = a$ and dr/dt is chosen = 0. The traverse time is the time at which $r = r_s$. The value of t_t is determined either by trial and error, solving Eq. (A41) numerically, or by solving numerically

$$\frac{d^2 t}{dr^2} = \frac{eq_s g}{M(r_s^3 - a^3)} \left[\frac{dt}{dr} \right]^3 \left[\frac{r_s^3}{r^2} - r \right] \left[1 - e^{-\frac{t}{\tau'}} \right]. \quad (\text{A43})$$

The results for $\tau' = \tau$ and for $\tau' = t_t > \tau$ are shown in rows 19 and 20 respectively of Table 3.